

Dynamic Modeling of Distributed Wear-Like Faults in Spur Gears: Simplified Approach with Experimental Validation

Lior Bachar¹, Roe Cohen¹, Omri Matania¹, and Jacob Bortman¹

¹*Department of Mechanical Engineering, Ben-Gurion University of the Negev, Beer-Sheva, 8410501, Israel*

*liorbac@post.bgu.ac.il
coroe@post.bgu.ac.il
omrimat@post.bgu.ac.il
jacobort@bgu.ac.il*

ABSTRACT

Dynamic models of gears are recognized for offering a promising platform for gaining a profound understanding of the dynamic response, particularly the vibration signature. Wear is considered among the most common and concerning fault mechanisms in gears, yet its recognition and subsequent diagnosis remain challenging. In this study, we introduce an existing dynamic model of spur gear vibrations and extend its validation for distributed wear-like faults. The novelty of this work lies in addressing the complexities associated with modeling distributed faults using simplified yet sophisticated approaches. These involve variance among defected teeth, calculation of time-variant gear mesh stiffness, and consideration of the forces induced by the fault. The model is validated through pioneering controlled experiments, analyzing dozens of degrading distributed wear-like faults. This comparison verifies our capability to generate realistic simulations of vibration signals from worn gears. To bridge the discrepancy between the induced and simulated faults, the model first constructs the healthy profile of the inspected gear, incorporating manufacturing errors and tooth modifications. Subsequently, meticulous photography enables the replication of faults in the model with a high resemblance to the experiment. The results demonstrate a strong correlation between measured and simulated signals, as verified through trend analysis of features extracted from synchronous average signals in both the cycle and order domains. This study lays the groundwork for in-depth investigation into the physics of gear wear, paving the way for potential applications such as fault severity estimation and intelligent fault diagnosis in future studies.

1. INTRODUCTION

Predictive maintenance of gear wear is crucial, considering gears' pivotal role in rotating machinery and their constant susceptibility to failure due to operation in harsh regimes. Gear fault types can be broadly classified into localized faults such as breakage and cracks, and distributed faults such as abrasive wear and fatigue pitting. Abrasive wear, caused by oil contamination and sliding motion, leads to continuous destruction of the tooth surface, posing a viable risk of catastrophic failure due to reduced gear efficiency and high stress concentrations. Nevertheless, Feng, Ji, Ni, and Beer (2023) reviewed the latest developments in gear wear monitoring and demonstrated that diagnosing gear wear through vibration analysis is still challenging due to the intricate patterns manifested in the signature that remain unresolved. Physical models, such as tribological models (Archard, 1953) and dynamic models (Liang, Zuo, and Feng, 2018; Mohammed & Rantatalo, 2020), have been suggested over the years in order to bridge this gap.

Most of the published dynamic models of gear wear typically analyze the effects of wear on the time variant gear mesh stiffness (gms). Liu, Yang, and Zhang (2016) utilize a spur gear model to study the changes in the gms and transmission error due to wear, as well as the wear expression in the vibrations. Brethee, Zhen, Gu, and Ball (2017) introduce a helical gear model, validated through endurance tests, and analyze both the gms and the increase in frictional excitation with wear. Many other studies (Chen, Lei, and Hou, 2021; Cui et al., 2023; Ren & Yuan, 2022; Shen et al., 2020), incorporate Archard's tribological model in the dynamic model to calculate the worn surface, demonstrating the effect of wear on the dynamic characteristics. However, most of these models lack experimental validation, and in general, the coefficients in Archard's equation are largely unknown, making their evaluation in the models nontrivial.

In this work, we introduce a novel approach for modeling distributed wear-like faults in spur gears, validated through

Lior Bachar et al. This is an open-access article distributed under the terms of the Creative Commons Attribution 3.0 United States License, which permits unrestricted use, distribution, and reproduction in any medium, provided the original author and source are credited.

experimentation. By leveraging simplifying assumptions, this modeling approach effectively captures the dynamic response of worn gears, while also facilitating its adaptation by other scholars in their models. In Section 2, we introduce the framework of the existing dynamic model, establishing the groundwork for this study. Section 3 delves into the simplified wear modeling approach, while Section 4 presents the experimental setup. Model validation is detailed in Section 5, accomplished through vibration analysis of the synchronous average signals and their spectrum. Finally, Section 6 concludes this work, providing insights and suggesting potential directions for future research.

2. DYNAMIC MODEL

This study adopts the dynamic model for spur gears proposed by Dadon, Koren, Klein, and Bortman (2018), which has been experimentally validated for healthy gears and various localized faults, serving as the foundation for this study. The simulated system has an open gearbox with torsional shafts connecting the driving pinion to a motor and the driven gear to a brake applying external torque, as illustrated in Figure 1. The vector of generalized coordinates (u) consists of 13 degrees of freedom: six for each wheel, representing linear displacement (x_i, y_i, z_i) and angular position (θ_i, ϕ_i, ψ_i) in space (where $i=p, g$), and another for the brake's angle (θ_b). Figure 2 presents a block diagram illustrating the model's stages. The vibration signal is generated by solving the Euler-Lagrange equations of motion, as described in Eq1.

$$M\ddot{u} + C\dot{u} + K(u) \cdot u = F(t, u) \quad (1)$$

Here, M, C, K , and F are the mass, damping, and stiffness matrices, and the excitation force vector, respectively. The non-linearity in $K(u)$ arises from the time-variant gear mesh stiffness (gms), computed using the potential energy method. The model is configured with parameters such as gear module, number of teeth, tooth width, and surface quality, alongside operational conditions like input speed and load. In contrast to many published models, where the gms is the sole non-linear component, this model introduces non-linearity in the excitation force vector. It incorporates deviations from the involute profile, such as surface roughness and faults, as displacement inputs along the Line of Action (LoA), which are subsequently transformed into forces by appropriately multiplying them with the gms . Thus, the excitation force consists of three components overall: the motor torque, the brake torque, and the force induced by displacements along the LoA, as shown in Eq. 2.

$$F = k_{\theta_p} \theta_m \cdot \hat{\theta}_p + T_b \cdot \hat{\theta}_b + gms \cdot \delta \cdot \bar{c} \quad (2)$$

Here, k_{θ_p} is the input shaft torsional stiffness, θ_m is the motor's angle, T_b is the brake's torque, δ is the displacement along the LoA, and \bar{c} is a vector of geometric coefficients projecting this force onto u . $\hat{\theta}_p$ and $\hat{\theta}_b$ are unit vectors pointing to θ_p, θ_b , respectively.

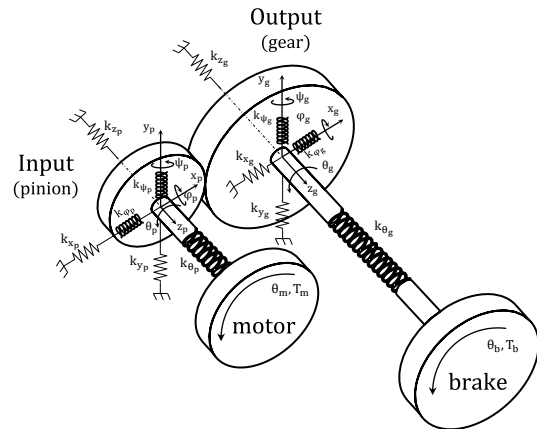


Figure 1. The simulated system (Dadon et al., 2018).

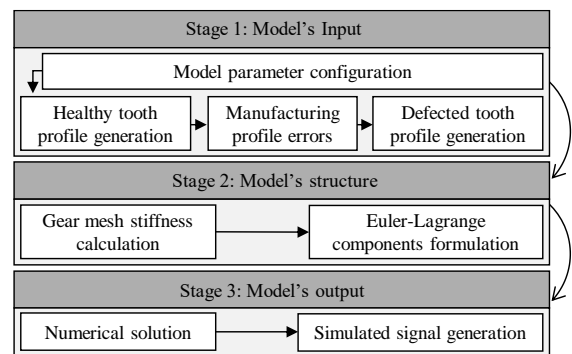


Figure 2. A schematic block diagram of the dynamic model.

3. GEAR WEAR MODELING

Any model development is grounded in premises that aim to balance the tradeoff between simplicity and reality (Mohammed & Rantatalo, 2020). We make the following assumptions that simplify our ability to simulate gear wear:

Assumption I: The worn profile is linear (or piecewise linear) and uniform along the tooth width, as illustrated in Figure 3.

Assumption II: The nominal parameters of the worn profile vary slightly among teeth.

Assumption III: The worn profile influences the cross-section properties of the tooth, thereby impacting the potential strain energy and, consequently, the gms .

Assumption IV: Contact properties such as contact ratio, pressure angle, and initial contact point remain unchanged. However, any deviation from the nominal LoA is treated as a displacement input in the excitation force.

It is crucial to acknowledge the limitations of these assumptions, as the gear wear mechanism is more complex, involving details not covered by these simplifications, such as sliding motion and improper contact. Nonetheless, these simplifications establish a foundation for comprehending the general wear behavior. The following subsections explore the effects of wear on the gms and the excitation force.

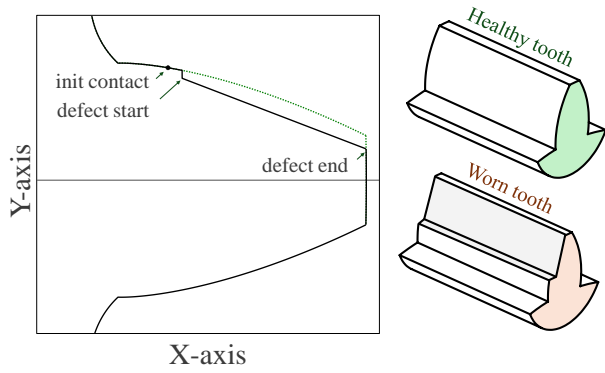


Figure 3. The simulated worn profile.

3.1. Effects of Wear on the Gear Mesh Stiffness

The computation of the gms commonly involves two steps, both are affected by wear. The first step employs the potential strain energy method for calculating the equivalent stiffness of a meshing tooth pair from engagement to separation. In this case, the influence of wear is self-evident, as tooth geometry is changed, and potential strain energy is derived from integration with respect to volume. The second step involves combining the equivalent stiffness of all tooth pairs based on the contact ratio governing the transition from a single pair to a double pair. In a healthy state, the equivalent stiffness can be computed once and then replicated and concatenated to form the cyclic gms. This procedure stays largely similar in case of localized faults, except for swapping the equivalent stiffness of one healthy pair with that of the defected pair. However, with distributed wear faults, where the worn profile varies among teeth, the equivalent stiffness is calculated individually for each tooth pair, and then meticulously combined, as depicted in Figure 4.

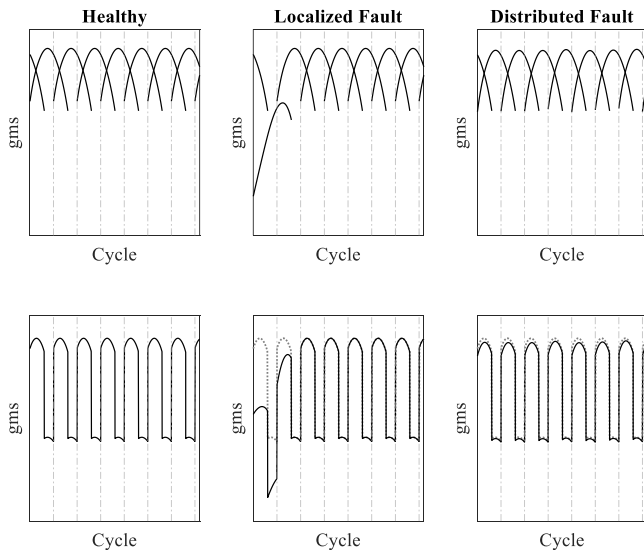


Figure 4. Construction of the gms signal in case of a healthy status, localized fault, and distributed fault.

3.2. Effects of Wear on the Excitation Force

One of the non-trivial assumptions made is that contact properties remain wear-invariant. While this assumption may be controversial, it is not without basis when appropriately compensated. As explained previously, deviations from the LoA are treated as displacement inputs in the excitation forces. The computation of the fault displacement involves straightforward geometric manipulations according to Eq. 3, using parameters depicted in Figure 5. Given that the fault displacement is unique for each tooth, it is multiplied by the equivalent stiffness of its corresponding pair, and the resulting product is then combined using the same procedure as in the gms, as depicted in Figure 6.

$$\delta_{\text{fault}} = (Y_{\text{invlt}} - Y_{\text{def}}) \cdot \frac{\cos(\gamma)}{\cos(\phi + \gamma)} \quad (3)$$

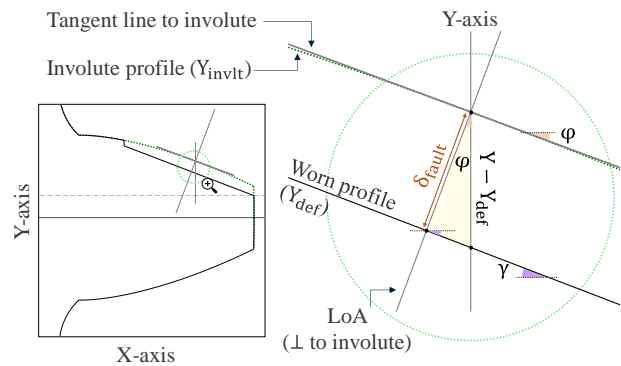


Figure 5. An illustration of the fault displacement calculation and the required parameters.

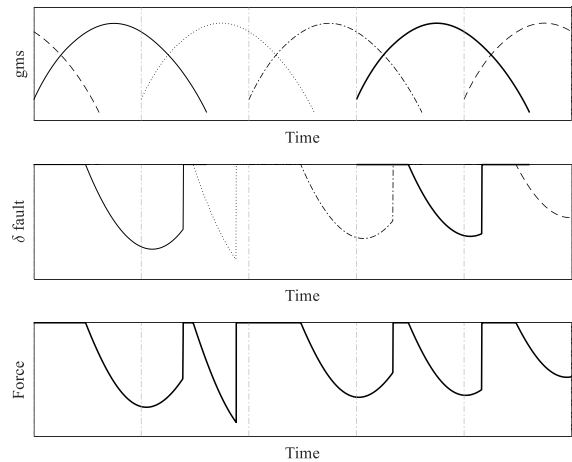


Figure 6. Generation of excitation force through fault displacement along the LoA, multiplied by the gms.

4. EXPERIMENTAL SETUP

We conducted an extensive controlled experiment for model validation, employing a dedicated test apparatus for spur gears. Vibration data were collected for both a healthy (H) status and 35 degrading wear cases (W_i), using piezoelectric

accelerometers, alongside rotational speed measured by tachometers, as depicted in Figure 7. Details regarding the experimental program and gearbox parameters can be found in Table 1. The degradation of a reference tooth throughout the experiment is showcased in Figure 8. This figure includes photographs illustrating three cases corresponding to the beginning, middle and the end of the experiment. Additionally, a heatmap depicts the contour of all wear cases, with the color gradient correlating with fault severity.

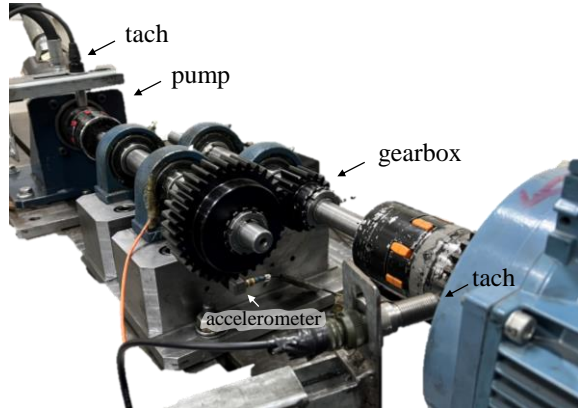


Figure 7. The experimental setup employed for validation.

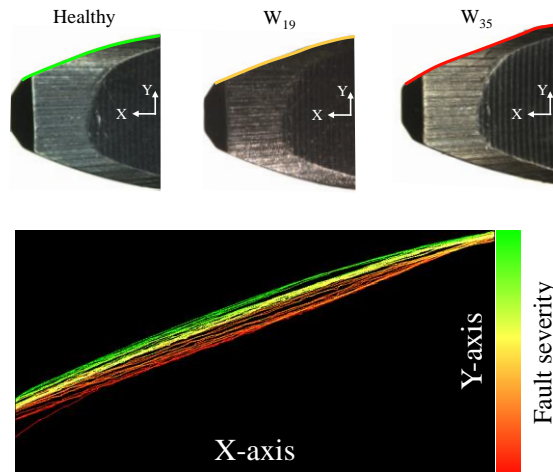


Figure 8. Photographs and heatmap depicting the profile degradation of a reference tooth throughout the experiment.

Table 1. Gearbox parameters and experimental program.

Gearbox parameters	
Module	3mm
Reduction ratio	35:18
Precision grade	DIN8
Experimental program	
Input speed	15rps, 45rps
Output Load	10Nm
Sampling rate	50kS/s
Signal duration	60s
Health status	H, {Wi} _{i=1} ³⁵

5. MODEL VALIDATION

The validation of the proposed wear modeling approach is empirical, relying on a qualitative comparison between simulation and experiment. This comparison involves analyzing trends in energy-based (such as rms) and shape-based (such as kurtosis) features extracted from the synchronous average (SA) signal and the difference signal in the cycle domain, and the SA spectrum in the order domain (Matania, Bachar, Bechhoefer, and Bortman, 2024). For both simulated and measured data, the SA is computed after the raw vibration signal undergoes angular resampling based on the output shaft’s speed. It is essential to note that while the simulated signal is directly calculated at the wheels’ center, the measured signal is significantly influenced by the transmission path between the gearbox and the sensor. This influence results in expected differences in spectral behavior, such as attenuations and resonances (Bachar et al., 2021, 2023). Consequently, experimental and simulated results are presented with left and right y-axes, with energy-based features normalized by the healthy (H) status according to Eq. 4, ensuring comparability of general trends.

$$F_{norm} = \frac{|F - F_H|}{F_H} \quad (4)$$

5.1. SA Analysis in the Cycle Domain

Figure 9 compares SA signals at 45rps in healthy status and for severe wear. Expected impulses appear in all the SAs. Both experiment and simulation show an amplified signal without sharp and rare impulsive responses due to wear, as expected. This observation highlights challenges in wear monitoring, as faulty signals may not emphasize the fault, creating a false impression of a healthy transmission.

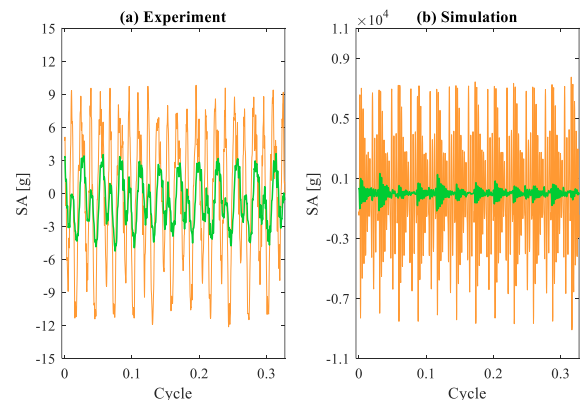


Figure 9. Comparison of SA signals between simulation (right) and experiment (left) at 45rps, in healthy (green) and severe wear (orange) statuses.

Figure 10 analyzes trends in SA rms, difference rms, and difference kurtosis across fault severity. Experimental results are depicted with error bars representing the scattering in the feature values. The following insights can be derived from these results:

- There is a strong correlation between simulation and experiment in rms trends, particularly evident in difference rms, where rms increases monotonously with wear degradation. Moreover, the "wavy" trend is observable in both simulation and experiment, suggesting that this behavior may have a physical basis.
- The higher speed (45rps) exhibits superior correlation between simulation and experiment. The purportedly weaker correlation at 15rps may be attributed more to the effects of speed and transmission path on the vibration signature (Bachar et al., 2021) rather than discrepancies.
- Kurtosis values are generally low and remain relatively stable. Given that kurtosis emphasizes sharp, rare impulses, which distributed wear faults are not expected to, it might not be suitable for gear wear monitoring. This insight is evident both in simulation and experiment.
- In most cases, discrepancies between simulation and experiment are more evident in more severe faults.

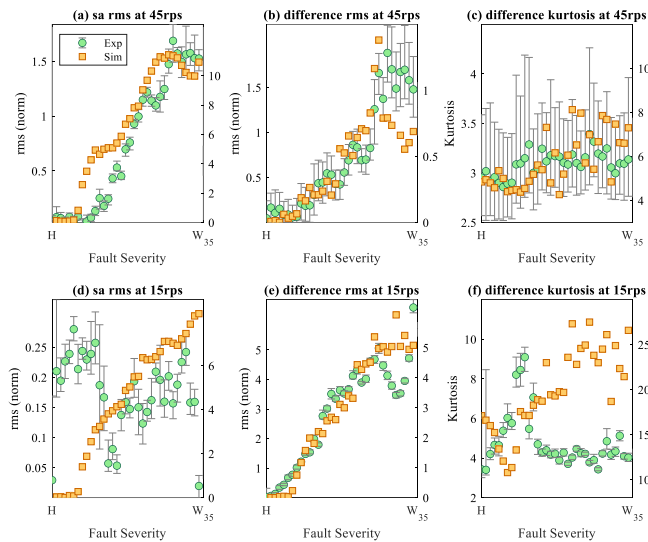


Figure 10. Trend analysis of features extracted from the SA and difference signals across fault severity at 45rps (top row) and 15rps (bottom row).

5.2. SA Analysis in the Order Domain

A comparison of the SA spectra across fault severity is presented in the spectrograms in Figure 11. For clarity, the top row in each spectrogram, corresponding to the healthy status (H), is thicker and separated from the degrading wear cases by a line. High amplitudes at the gearmesh harmonics are observed in all spectra, as expected. Furthermore, across both speeds and for both simulation and experiment, the general behavior with respect to fault severity is similar; that is, the spectral energy mostly varies monotonously with health degradation. However, the optimal wear manifestation for fault detection and degradation monitoring varies across

different frequency bands for each combination of data source and rotational speed, as expected. The differences in spectrum background are expected to lead to such discrepancies, but as long as they are acknowledged, focus can be placed on the similarities obtained between experiment and simulation.

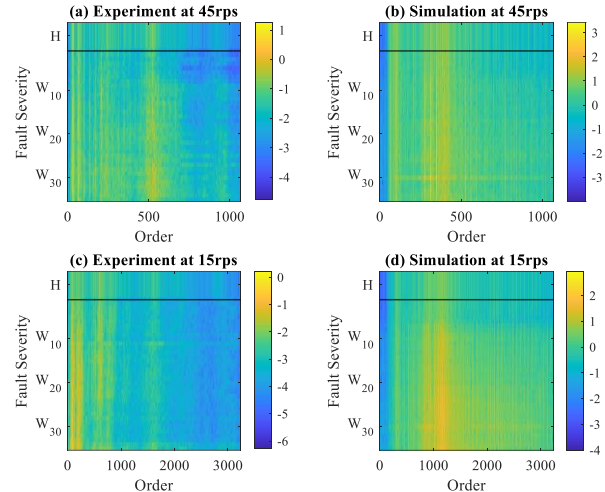


Figure 11. SA spectra across fault severity between experiment (left) and simulation (right) at 45rps (top) and 15rps (bottom).

Early research on gear monitoring (Randall, 1982) demonstrates the impact of distributed wear faults on gear mesh harmonics and modulation sidebands in the spectrum. To capture similar behaviors between simulation and experiment, we compute the gear mesh energy (gme) and modulation sideband energy (sbe) in the spectrum (X) according to Eq. 5-6 and compare their trends across fault severity, as depicted in Figure 12.

$$gme = \sum_{n=1}^{gm_{max}} |X(gm \times n)| \quad (5)$$

$$sbe = \sum_{n=1}^{gm_{max}} \sum_{m=1}^{gm/2} |X(gm \times n \pm m)| \quad (6)$$

Here, gm_{max} is the maximum number of gearmesh harmonics available within bandwidth. The following insights can be derived from the spectral analysis results:

- There is a strong correlation between simulation and experiment in both gme and sbe trends, closely mirroring the energy-based feature analysis in the cycle domain in Figure 10.
- Both spectral energies exhibit a monotonic variation with wear degradation, displaying the same "wavy" trend as discussed in the cycle domain analysis.

The spectral analysis aligns with the feature analysis in the cycle domain, confirming the similarity between simulated

and measured signals. Despite relying on a set of non-trivial assumptions, the proposed simplified modeling approach successfully captures the general wear patterns in the simulated signal. Moreover, while features for monitoring localized faults focus mainly on signal shape and modulation sidebands, gear mesh energy is also crucial for diagnosing wear faults. This holds true in both simulation and experiment across different speeds. Discrepancies between simulation and experiment, stemming from the assumptions made, are more pronounced in severe wear faults, as expected due to the challenging assumption of invariant contact properties with wear. Nevertheless, the strong similarities between simulation and experiment validate the model's ability to generate a simulated vibration signal reflecting the fundamental characteristics of gear wear.

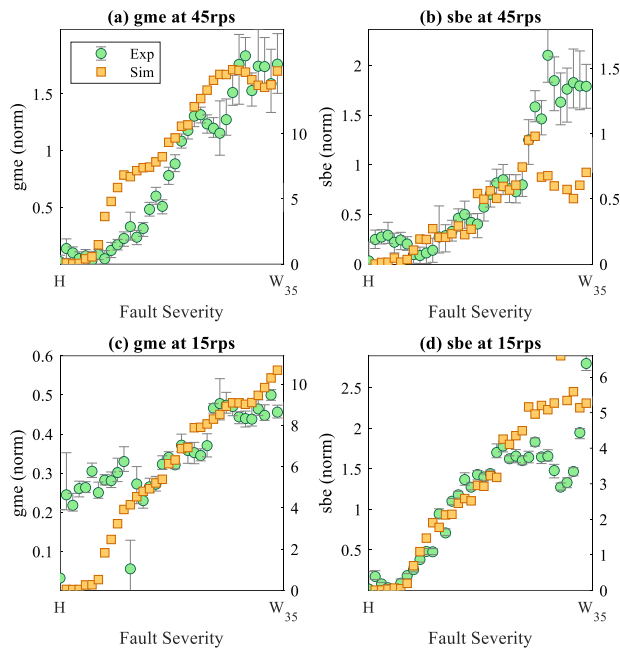


Figure 12. Comparison of spectral analysis of the gme (left) and sbe (right) between simulation and experiment at 45rps (top row) and 15rps (bottom row).

6. CONCLUSION

Gear wear monitoring is crucial for predictive maintenance, yet identifying patterns in the vibration signature associated with wear remains challenging. This study aims to bridge this gap by introducing a novel, simplified approach for simulating distributed wear-like faults. We make a set of assumptions to investigate wear characteristics essential for health monitoring, incorporating wear faults into an existing framework of dynamic model for gear vibrations. We demonstrated the impact of wear on the non-linear gear mesh stiffness and the excitation force according to the proposed modeling. Extensive controlled experiments validate our approach, comparing experimental and simulated results

across different speeds and fault severities. A visual examination of the synchronous average signal and its spectrum across fault severity confirms that the proposed wear modeling closely resembles the experimental results, yielding similar insights. In-depth trend analyses of features in both cycle and order domains reveal crucial insights into the intricacies of wear monitoring, capturing "wavy" trends as the fault deteriorates. This underscores the importance of analyzing energy-based features, such as gear mesh energy and sideband energy, rather than shape-based features, for monitoring distributed wear faults. The strong correlation between experimental and simulated results confirms the feasibility of our approach, suggesting it as a simple yet effective enhancement for simulating wear faults in any standard dynamic gear model. Our study opens avenues for practical applications, including refining the simplified model for real-system applications and developing novel methods for wear prediction in future work.

REFERENCES

- Archard, J. F. (1953). Contact and Rubbing of Flat Surfaces. *Journal of Applied Physics*, 24(8), 981–988. <https://doi.org/10.1063/1.1721448>
- Bachar, L., Dadon, I., Klein, R., & Bortman, J. (2021). The effects of the operating conditions and tooth fault on gear vibration signature. *Mechanical Systems and Signal Processing*, 154, 107508. <https://doi.org/10.1016/j.ymssp.2020.107508>
- Bachar, L., Matania, O., Cohen, R., Klein, R., Lipsett, M. G., & Bortman, J. (2023). A novel hybrid physical AI-based strategy for fault severity estimation in spur gears with zero-shot learning. *Mechanical Systems and Signal Processing*, 204. <https://doi.org/10.1016/j.ymssp.2023.110748>
- Brethee, K., Zhen, D., Gu, F., Theory, A. B.-M. and M., & 2017, undefined. (2017). Helical gear wear monitoring: Modelling and experimental validation. *ElsevierKF Brethee, D Zhen, F Gu, AD BallMechanism and Machine Theory*, 2017•Elsevier. <http://dx.doi.org/10.1016/j.mechmachtheory.2017.07.012>
- Chen, W., Lei, Y., Fu, Y., theory, L. H.-M. and machine, & 2021, undefined. (2021). A study of effects of tooth surface wear on time-varying mesh stiffness of external spur gear considering wear evolution process. *ElsevierW Chen, Y Lei, Y Fu, L HouMechanism and Machine Theory*, 2021•Elsevier. <https://doi.org/10.1016/j.mechmachtheory.2020.104055>
- Cui, Q., Dong, N., Cui, Q., Tong, J., Wang, R., Lu, H., Dong, N., Zhou, J., Tong, R., Wang, H., & Lu, F. (2023). Study on wear evolution of spur gears considering dynamic meshing stiffness. *Springer*, 37(7), 2023. <https://doi.org/10.1007/s12206-023-0606-3>

- Dadon, I., Koren, N., Klein, R., & Bortman, J. (2018). A realistic dynamic model for gear fault diagnosis. *Engineering Failure Analysis*, 84. <https://doi.org/10.1016/j.engfailanal.2017.10.012>
- Feng, K., Ji, J. C., Ni, Q., & Beer, M. (2023). A review of vibration-based gear wear monitoring and prediction techniques. In *Mechanical Systems and Signal Processing* (Vol. 182). <https://doi.org/10.1016/j.ymsp.2022.109605>
- Liang, X., Zuo, M. J., & Feng, Z. (2018). Dynamic modeling of gearbox faults: A review. *Mechanical Systems and Signal Processing*, 98, 852–876. <https://doi.org/10.1016/J.YMSSP.2017.05.024>
- Liu, X., Yang, Y., International, J. Z.-T., & 2016, undefined. (2016). Investigation on coupling effects between surface wear and dynamics in a spur gear system. *ElsevierX Liu, Y Yang, J ZhangTribology International*, 2016•Elsevier. <https://doi.org/10.1016/j.triboint.2016.05.006>
- Matania, O., Bachar, L., Bechhoefer, E., & Bortman, J. (2024). Signal Processing for the Condition-Based Maintenance of Rotating Machines via Vibration Analysis: A Tutorial. *Sensors 2024, Vol. 24, Page 454, 24(2)*, 454. <https://doi.org/10.3390/S24020454>
- Mohammed, O. D., & Rantatalo, M. (2020). Gear fault models and dynamics-based modelling for gear fault detection – A review. *Engineering Failure Analysis*, 117, 104798. <https://doi.org/10.1016/J.ENGFAILANAL.2020.104798>
- Randall, R. B. (1982). A New Method of Modeling Gear Faults. *Journal of Mechanical Design*, 104(2), 259–267. <https://doi.org/10.1115/1.3256334>
- Ren, J., Coatings, H. Y.-, & 2022, undefined. (2022). A dynamic wear prediction model for studying the interactions between surface wear and dynamic response of spur gears. *Mdpi.ComJ Ren, H YuanCoatings*, 2022•mdpi.Com. <https://doi.org/10.3390/coatings12091250>
- Shen, Z., Qiao, B., Yang, L., Luo, W., Yan, R., Manufacturing, X. C.-P., & 2020, undefined. (2020). Dynamic modeling of planetary gear set with tooth surface wear. *ElsevierZ Shen, B Qiao, L Yang, W Luo, R Yan, X ChenProcedia Manufacturing*, 2020•Elsevier. <https://doi.org/10.1016/j.promfg.2020.06.010>
- AI applications. Lior completed with honors his bachelor's degree and master's degree in mechanical engineering in Ben-Gurion University of the Negev.
- Roe Cohen** is currently a Ph.D. student in BGU-PHM LAB in the department of mechanical engineering in Ben-Gurion University of the Negev, under the supervision of Prof. Jacob Bortman. Roe completed with honors his bachelor's degree and master's degree in mechanical engineering in Ben-Gurion University of the Negev.
- Omri Matania** is currently a Ph.D. student in BGU-PHM LAB in the department of mechanical engineering in Ben-Gurion University of the Negev, under the supervision of Prof. Jacob Bortman. Omri is a Talpiot graduate and served nine years in IDF in several roles including algorithm section leader. He completed with honors his bachelor's degree in mathematics and physics in the Hebrew University of Jerusalem and completed his master's degree with honors in mechanical engineering in Ben-Gurion University of the Negev
- Jacob Bortman** is currently a full Professor in the department of mechanical engineering and the head of the PHM Lab in Ben-Gurion University of the Negev. Retired from the Israeli air force as brigadier general after 30 years of service with the last position of the head of material directorate. Chairman and member of several boards: director of business development of Odysight Ltd, Chairman of the board of directors, Selfly Ltd., board member of Augmentum Ltd., board member of Harel finance holdings Ltd., Chairman of the board of directors, Ilumigyn Ltd. Editorial board member of: "Journal of Mechanical Science and Technology Advances (Springer, Quarterly issue)". Head of the Israeli organization for PHM, IACMM - Israel Association for Comp. Methods in Mechanics, ISIG - Israel Structural Integrity Group, ESIS - European Structural Integrity Society. Received the Israel National Defense prize for leading with IAI strategic development program, Outstanding lecturer in BGU, The Israeli prime minister national prize for excellency and quality in the public service - First place in Israel. Over 80 refereed articles in scientific journals and in international conference.

BIOGRAPHIES

Lior Bachar is currently a current Ph.D. student in mechanical engineering in BGU-PHM LAB at Ben-Gurion University of the Negev, Beer-Sheva, Israel. His primary academic interest is vibration-based diagnosis of gears. His research, published in numerous papers, employs hybrid physical data-driven based approaches, integrating experimentations, signal processing, dynamic modeling, and